An Assessment of Design Criteria for Continuous-Welded Rail on Elevated Transit Structures

DONALD R. AHLBECK, ANDREW KISH, and ANDREW SLUZ

ABSTRACT

For a safe, economical design, three basic problems must be addressed in the use of continuous-welded rail (CWR) on aerial structures: (a) the control of stresses in the rail caused by differential longitudinal movements between the rail and superstructure (deck, girder) attributed to temperature changes or other causes, (b) the control of rail-break gap size and the resulting loads into the superstructure caused by a pull-apart, and (c) the transfer of loads and moments from the superstructure into the substructure (i.e., columns and piers). These are conflicting design goals, however, and the ideal solution to one may worsen the problem with another. Design compromises are necessary to attain acceptable loads, component stresses, and deflections under all expected conditions. In this paper, the existing design criteria for use of CWR on elevated transit structures are reviewed and evaluated. Available literature (e.g., reports, codes, and specifications) is reviewed; and visits to five of the newer U.S. transit properties are described, discussing design philosophies, past experience, and current maintenance practices. Simple iterative computer models were developed to provide estimates of thermally induced loads into the rail and structure, and rail-gap size and loads caused by a pull-apart, as a function of nonlinear fastener characteristics and structure configuration. Results of analyses of typical transit structures employing these models are described in the paper.

As part of the technical support that the Transportation Systems Center (TSC) has provided to UMTA under the Urban Rail Rehabilitation, Construction, and Maintenance Program (UM-476), investigations have been conducted to develop safe and cost-effective means to improve the performance of elevated transit structures. The primary objectives of these investigations were to develop methods and techniques for assessing the structural integrity of transit track and elevated structures, and to determine if current design criteria, specifications, rehabilitation requirements, and maintenance practices are adequate to ensure structural integrity.

One of these investigations (1) addressed the technical and economic factors in the use of continuous-welded rail (CWR) on elevated structures. The replacement of bolted-joint rail (BJR) with CWR on elevated transit structures would reduce the maintenance and noise problems caused by wheel/rail impact loads at the rail joints. However, large variations in temperatures over daily or seasonal cycles can generate large lateral and longitudinal loads in the track because of thermal expansion or contraction. In BJR, the rail joints provide for slippage that will reduce these forces. With CWR, on the other hand, these locked-in thermal loads can damage the supporting structure if not properly handled. The older aerial track structures were not designed for CWR use, however, and the current practice of rail replacement on these older elevated structures is to continue the use of BJR. On newer elevated transit structures, CWR is more commonly used. However, the design criteria used to ensure overall structural integrity are varied, and there is a need to evaluate these criteria to determine if the resulting designs are adequate.

D.R. Ahlbeck, Battelle Columbus Division, 505 King Avenue, Columbus, Ohio 43201. A. Kish and A. Sluz, Transportation Systems Center, U.S. Department of Transportation, Kendall Square, Cambridge, Mass. 02142.

BACKGROUND

A general review of design criteria and standards for designing elevated structures for urban rail transit systems is provided in a report by Harrington (2). A major conclusion of this report was that the various criteria are similar enough that a uniform set of industry-wide standards is feasible. However, these design criteria do not explicitly address the use of CWR on elevated structures. There are no specific guidelines for rail restraint, nor established limits on the size of a rail gap that would result from a thermally induced rail break.

Current guideway design criteria also have been reviewed and compared by Dorton and Grouni (3,pp.134-144). Design methods more specific to the application of CWR to aerial transit structures are found in feasibility and design studies for the newer transit properties (4-7). Systems described in these reports range from California's Bay Area Rapid Transit (BART), the oldest of the modern U.S. transit systems (4), to the Vancouver, British Columbia, Advanced Light Rapid Transit (ALRT) system (5). A conference paper by Fox (8) discusses the design philosophy used in the Washington (D.C.) Metropolitan Area Transportation Authority (WMATA) steel bridge structures.

A recent paper prepared for the American Public Transit Association (APTA) Track Construction and Maintenance Subcommittee by Robert E. Clemons (elsewhere in this Record) specifically addresses the problems of CWR on aerial structures. In this paper (Continuous Welded Rail on BART Aerial Structures),

the concepts of direct fixation of rail to structure, the types of fasteners used, and the rail/structure interactions are discussed in detail. The three basic methods for accommodating thermally induced differential movements between rail and structure are described in this paper as follows: (a) elastic fasteners with nonslip rail clamps and rail/girder motion within the shear deflection of the fastener (used by BART); (b) elastic fasteners with controlled-slip rail clips providing elastic deformation to the longitudinal force limit of the clips [used by the Metropolitan Atlanta Rapid Transit Authority (MARTA), the Metro Dade Transportation Administration (MDTA), and the Maryland Mass Transit Administration (MTA-Baltimore)]; and (c) elastic fasteners with nonslip (or high slip-limit) rail clamps near the fixed end of each girder, and controlled-slip (low slip-limit) rail clips on the rest of the girder, where greater relative movement is expected (used by WMATA).

In summary, these reviews of current published design criteria and standards showed that the problems in the application of CWR to elevated transit structures are not specifically addressed. A review of the technical reports and design studies showed that different organizations have taken substantially different engineering approaches in handling these problems.

TRANSIT PROPERTY SITE VISITS

Five transit properties were visited during the course of this study (1) to (a) provide a firsthand look at the track and aerial structures; (b) interview system design engineers and track maintenance personnel; and (c) gather available material on design criteria, standards, and methods. These properties were as follows:

- MARTA,
- MTA-Baltimore,
- MDTA Metrorail,
- BART, and
- WMATA.

(Note that summaries of track, fastener, and aerial structure characteristics for these five systems are given in Table 1.)

The newer transit systems have followed different design philosophies in their utilization of CWR and direct-fixation (DF) fasteners on aerial structures. In an effort to control thermally induced stresses in the rail and loads into the structure, yet limit the rail-gap size in the event of a rail break, the different transit properties have used combinations of low- and high-restraint fasteners (WMATA), medium-restraint fasteners (MARTA, MDTA Metrorail, MTA-Baltimore), and high-restraint fasteners (BART).

BART has had little trouble with the high-restraint fasteners, and no evidence of excessive loads into the aerial structures. Rail gaps from the few rail breaks have been controlled to less than 1 in. WMATA, on the other hand, has experienced problems with its fasteners (9,10); and a few rail breaks have generated gap widths in excess of 6 in. Limited service experience has been accumulated on the newest systems that utilize the medium-restraint fasteners, but these fasteners have performed well to date.

EVALUATION OF CWR DESIGN CRITERIA

Three basic problems must be addressed in the design of aerial structures for use with CWR track:

1. The control of stresses in the rail attributed to differential longitudinal motions between the rail and superstructure because of temperature changes or other causes,
2. The control of rail-break gap size and resulting loads into the superstructure attributed to aerial pull-apart, and
3. The transfer of superstructure loads and moments into the substructure (e.g., piers and bents).

A solution to one of these problems may conflict with the ideal solution to another; therefore, design compromises must be made that will result in acceptable levels of component load, stress, and deflection under all expected conditions.

Longitudinal loads are developed between the CWR and the superstructure (i.e., deck and girders) of an aerial transit structure by differential movement and shear of the fasteners. Reaction loads are carried into the substructure (i.e., columns, piers, and bents) through fixed bearings and by shear or friction through expansion bearings. On curved track, lateral components of the longitudinal loads must also be reacted by the structure.

When the rail temperature drops many degrees lower than the rail neutral (stress-free) temperature, high-tensile, locked-in loads are developed. If a rail breaks, this tensile load is released. The load is distributed through rail fasteners in each direction from the point of break to points where the

TABLE 1 Track and Aerial Structure Characteristics for Representative North American Transit Systems

System	Rail Size	Rail Expansion Joints	Typical Fastener Type	Fastener Spacing (in.)	Elastomeric Pad Thickness (in.)	Rail Clip	Fastener Stiffness (kips/in.)[b] Vertical	Lateral	Longitudinal
MARTA	115 RE	None	Hixson H-10, Landis/ Pandrol, Hixson H-15 (mod)	30	3/4	Bolted clamp Spring clip Spring clip	130-300[a]	32-	10-40
MTA-Baltimore	115 RE	Special trackwork	Hixson H-15A	36	5/8	Spring clip	120-180	38-	8-50
MDTA Metrorail	115 RE	None	Landis/Pandrol	30	3/4	Spring clip	80-120	20-	10-[c]
BART	119 CF&I	None	Landis/Pandrol, Hixson	30-36	3/4	Bolted clamp	250-400[a]	24-33	18-36
WMATA	115 RE	None	Landis/Pandrol, Hixson, Lord	30	3/4	Bolted clamp	80-130	32-44	12-47

Note: PCC = precast concrete and CIPC = cast-in-place concrete; for span type: simple = single span as opposed to continuous (spans tied together) and floating = E-E/E-E bearing arrangement (see Figure 1B, righthand span); and for fastener type: nonslip = no expetted rail/fastener movement and slip = intentional (expected) rail/fastener movement.

[a] Some stiffening with age is assumed.
[b] Fastener stiffness = applied load divided by rail/baseplate relative motion in axis of load (lateral and longitudinal stiffnesses measured under vertical loading, except BART).
[c] No maximum stiffness specified.
[d] For rail stress calculations.

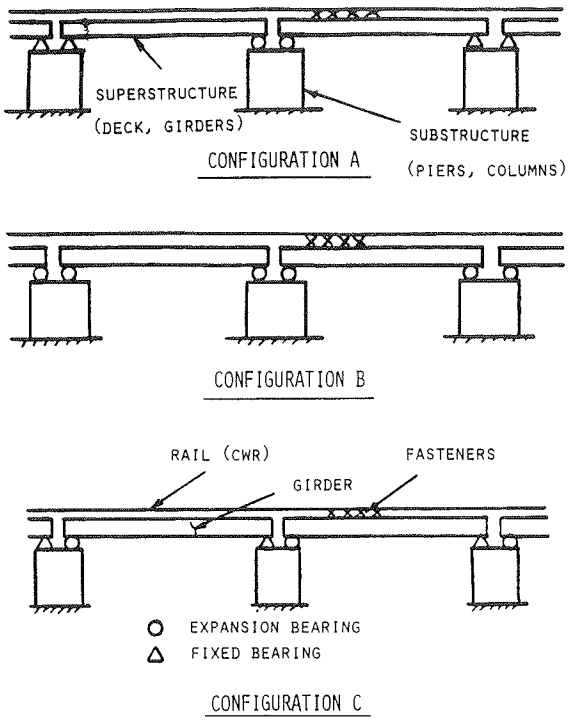

FIGURE 1 Bearing configurations for elevated structure girders.

thermal tensile load is again sustained in equilibrium.

Part of the load from a broken rail is transferred to the unbroken rail(s) of the guideway, and part is transferred to the substructure through fixed and expansion bearings. The exact magnitudes of these loads depend strongly on the substructure (bent or column) longitudinal stiffness, the structure-bearing configuration, and the rail fastener restraint characteristics.

The effects of column and girder bearing stiffnesses depend on the specific bearing configuration used in the structure. Three common configurations used with aerial transit structures are shown in Figure 1. The first of these (A) is a symmetrical arrangement common to modern transit systems such as BART. The second configuration (B), also symmetrical, is used on the level track sections of the MDTA system. The third configuration (C) is an asymmetrical arrangement commonly used on railroad and highway bridges.

Rail Stresses

An analysis of rail stresses must include contributions of vehicular and structural loads, as well as the thermally induced stresses. Current transit track design practice uses the factors recommended by the Association of American Railroads (AAR) when rail bending stress is calculated (11). Starting with the maximum bending stress under the peak expected dynamic wheel load, these factors account for contributions attributed to lateral bending, track condition, rail wear and corrosion, and unbalanced superelevation. Additional components can include

- Stress caused by acceleration or braking of vehicles,
- Stress in rail caused by bending of superstructure,
- Axial stress caused by composite-beam bending, thus inducing shear in fasteners and load into rail, and
- Stress caused by rail or structure interaction force (or both) through fasteners.

The total of these stresses plus the maximum expected temperature-induced stress is subtracted from the yield stress of the rail. This difference, reduced by a suitable factor of safety, will establish the maximum design stress resulting from differential movement between rail and superstructure. From two recent design studies (6,7), the following rail stress contributions were expected:

- Bending stress (all sources, multiplied by the factor of safety): 37 to 40 percent of yield stress;
- Thermal stress: 17 to 18 percent of yield stress; and
- Rail or structure differential movement, or both: 26 to 29 percent of yield stress.

Several methods are used to calculate the load generated in the rail by thermally induced movement of the superstructure (girders or deck). One method assumes a constant fastener restraint per unit length over the total span length. This is conservative (i.e., the calculated load is higher than the actual load), and not too inaccurate for low- to

Longitudinal Restraint Load (max., aerial, lb)		Aerial Structure Total Length	Span Length (ft)			Aerial Structure		Span Type	Rail-Laying Temperature (°F)	Expected Temperature Range (°F)	
Nonslip	Slip		Typical	Min.	Max.	Girder	Deck			Structure	Rail
10,000	2,000-3,000	4,658 (ft)	70	70	130	Steel	PCC	Floating	80		±70
–	1,200-1,600	10,500 (ft)	85	65	95	PCC unit		Simple	80		
–	1,540-2,400	20.8 (mi)	80	40	110	PCC unit		Floating	60-80	±60	±60
10,000-15,000	–	9 (mi)	70		100	PCC unit		Simple	60-80	±30	±50
7,000-10,000	250-750	3,090 (ft)	80	63	107	Steel	CIPC	Simple	55-75		-90[d]

medium-restraint fasteners. Another method assumes a linearly decreasing fastener load over the length of the span, based on fastener shear stiffness and the maximum thermal movement at the expansion end of the span. This method assumes that the fastener shear force does not exceed the slip limit force of the fastener, and is therefore accurate only for high-restraint fasteners. A much better solution is made possible by including the slip-limit force, up to the point where the linearly decreasing shear force drops below this force limit.

Over the span length of a girder, the rail is a relatively flexible element when compared with the girder itself. A small computer program was set up during this study to calculate fastener loads into the rail, assuming the rail to be a number of finite flexible elements between individual fasteners, rather than the rigid rail of the previously cited methods. An iterative solution is necessary, but the solution converges quickly (5 or 6 iterations), and the program can be run on a desk-top computer. Total loads between the rail and superstructure over one 80-ft span were calculated for three representative cases: a high-restraint fastener (BART), a medium-restraint fastener (MARTA, MDTA-Metrorail), and a low-restraint fastener (WMATA). Loads computed for a flexible rail are compared in Table 2 with loads calculated from the three cited rigid-rail methods. An important point in considering the rail flexible, however, is that the total load into the rail is distributed so that less than 70 percent of this load is reacted at the expansion end of the span at the highest-stressed point in the rail. This peak

TABLE 2 Comparison of Methods for Estimating Total Longitudinal Load Between Rail and Superstructure

	Longitudinal Loads for Different Methods (lb)			
Fastener Restraint (slip, lb)	Constant Restraint	Linearly Decreasing Shear Load	Linearly Decreasing Plus Slip	Computed (flexible rail)
High (10,000)	320,000	166,000	165,000	134,000
Medium (2,500)	80,000	166,000	70,000	67,000
Low (750)	24,000	166,000	23,000	23,000

Note: The following conditions are assumed: F--E/E--F girder bearing configuration, 60° F temperature change, and an 80-ft span length.

rail stress is a function of fastener shear stiffness: the lower the stiffness, the lower the percentage of total load (down to 50 percent) reacted by the rail at the expansion end.

Control of a Rail Break

A rail break or pull-apart will occur when the thermally induced tensile force in the rail attributed to a large drop in temperature exceeds the ultimate tensile strength of the rail. A pull-apart will most probably occur at or near an expansion joint in the superstructure (deck or girders), but the actual location of the break will be at a bad weld, rail flaw, or other weak spot.

Controlling a rail break presents two distinct problems demanding a somewhat opposite solution: (a) for safety reasons, the length of the rail-break gap must be minimized to reduce the possibility of derailment if train wheels pass over the break, and (b) the forces and moments into the superstructure attributed to the release of the locked-in thermal load must be minimized. The first requires higher fastener longitudinal restraint limits, and the second requires lower restraint limits.

The rail-break gap size is generally estimated by an equation in the form:

$$G = 2\ (X_{C1} + X_{C2} - X_{C3}) \tag{1}$$

where

$X_{C1} = P_{fns}/K_f$, the maximum longitudinal deflection of the "nonslip" fastener;
$X_{C2} = \alpha \Delta T L_s$, the nominal rail contraction;
$X_{C3} = (n_s P_{fs} + n_{ns} P_{fns}) L_s / 2 A_r E_r$, the reduction in rail contraction caused by fastener constraint;
α = coefficient of expansion, $6.5(10)^{-6}$ in./in.-°F for steel;
ΔT = temperature change, °F;
L_s = length of span (fixed to expansion point);
P_{fns} = minimum longitudinal restraint force, nonslip fastener;
P_{fs} = minimum longitudinal restraint force, controlled-slip fastener;
K_f = fastener longitudinal stiffness (lb/in.);
n_{ns} = number of nonslip fasteners in span;
n_s = number of controlled-slip fasteners in span;
A_r = cross-sectional area of rail (11.25 $in.^2$ for 115 lb/yd RE rail, the most commonly used size in U.S. systems); and
E_r = rail modulus of elasticity, $30(10)^6$ $lb/in.^2$.

A simplified form of this was used in the MDTA Metrorail design, based on a length, L, "...either side of the break over which full rail anchorage is provided...," so that

$$G = (\alpha \Delta T)^2\ A_r E_r / R_f \tag{2}$$

where R_f is the longitudinal restraint per inch of rail in pounds per inch.

To check the validity of these approximate methods, a finite-element model of the track structure was used with some typical system parameters given in Table 3. This model, called TBTRACK, has been

TABLE 3 Test Cases Run in Parameter Variation Study

Case	Stiffness (lb/in.)	Restraint (lb)	Limits (lb)	Description
1	30,000	2,500		Spring clip (MARTA, MDTA)
2	30,000	1,250		Spring clip, worn
3	10,000	1,250		Spring clip, worn
4	30,000	10,000		Bolted clamp (BART)
5	100,000	2,500		Stiff pad, spring clip
6	30,000	250	2,500	Low-slip, loose clamp
7	30,000	750	2,500	Medium slip, loose clamp
8	30,000	500	10,000	Nominal slip (WMATA)

used for several years to investigate the rail buckling phenomenon (13). The preceding equations for estimating the rail-break gap size assume linear load distributions. Results from the finite-element model, however, show the fastener load distributions to be nonlinear. Using the parameter values of Table 3, rail-break gap size for several cases as a function of temperature drops from the zero-stress (neutral) point are plotted in Figure 2.

The finite-element model is somewhat awkward and costly to run. Instead of completing the parametric study with TBTRACK, a simply iterative solution similar to that described in the previous section was developed. This model, called TRKTHRM, considers each rail element between fasteners as a spring, and

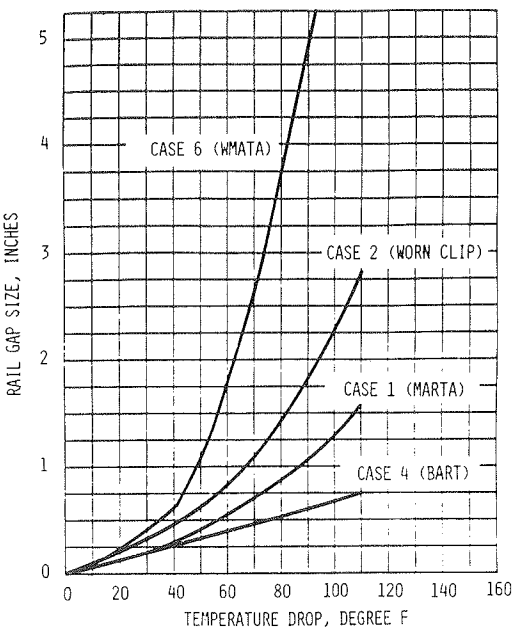

FIGURE 2 Rail-break gap size predicted by finite-element computer model.

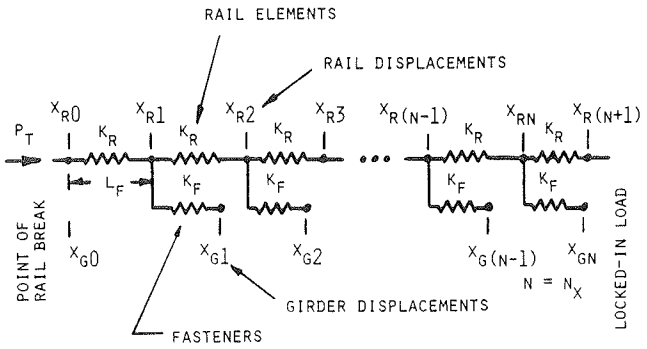

FIGURE 3 Model of broken rail on elevated transit structure.

each fastener as a bilinear spring with longitudinal slip (restraint limit). Girder displacements are inputs at one end of the fastener spring, with rail motions calculated for the other end.

Program TRKTHRM assumes that the rail breaks at the expansion joint, one spacing ahead of Fastener 1, and the locked-in thermal load must then be dissipated over an unknown number of fasteners. A first estimate of this number is calculated, just to start the iteration process. The solution moves in the appropriate direction to add or subtract fasteners until equilibrium with the locked-in load is achieved. The effects of girder contraction, which depend on the particular bearing configuration that is used (see Figure 1), are included in this model (see Figure 3).

The several methods for predicting rail-break gap size are compared in Table 4 with results from the two computer programs, TBTRACK and TRKTHRM. Note, first of all, that the finite-element model TBTRACK, with its limited number of lumped-fastener elements, tends to underestimate gap size. With medium-to-high fastener restraint, girder contraction increases gap size from 25 to 72 percent of that predicted if the girder does not contract. With low-restraint fasteners, girder contraction has little effect because movement is all in the slip zone. Equation 1 provides a reasonable estimate of gap size for medium-to-high-restraint fasteners, but badly underestimates gap size with low-restraint fasteners. Equation 2 provides a surprisingly accurate estimate in many cases, except where high-restraint fasteners are used.

Improved accuracy can be obtained with Equation 1 if the term X_{C2} is modified to use the estimated total number of fasteners over which the locked-in load is distributed so that

$$G = 2(X_{C1} + X_{C2} - X_{C3}) \quad (3)$$

where

$X_{C2} = 0.5\alpha\Delta T n_x L_s$;
$n_x = P_T/P_{fmax} = P_{fmax}K_r/2P_TK_f$;
$P_T = \alpha\Delta T A_r E_r$, the thermal load, lb;
$P_{fmax} = (n_{ns}P_{fns} + n_sP_fs)/(n_{ns} + n_s)$, the average fastener restraint limit, lb;
$K_r = A_rE_r/L_f$, the rail spring, lb/in.; and
K_f = fastener longitudinal stiffness, lb/in.

Limited data are available on rail-break gap sizes for specific fastener systems. Records of gap size and rail temperature are seldom kept. Rail breaks with high-restraint fasteners (e.g., BART and MARTA) have produced gaps of less than 1 in. The large gap sizes experienced by WMATA, on the other hand, may be induced by the dynamic stick-slip response of the rail in low-restraint fasteners.

Load Transfer Mechanisms

As discussed in the previous sections, longitudinal loads are developed between the CWR and the super-

TABLE 4 Comparison of Rail-Break Gap Size by Different Formulas

	Rail-Break Gap Size Estimates (in.)					
Case	Equation 1	Equation 2	Equation 3	TBTRACK ΔTg = 0	TRKTHRM ΔTg = 0	TRKTHRM ΔTg = 60
1	0.69	0.62	0.83	0.55	0.74	0.67
2	0.72	1.23	1.35	0.85	1.29	1.31
3	0.89	1.23	1.55	0.97	1.38	1.47
4	0.51	0.15	0.99	0.40	0.50	0.79
5	0.57	0.62	0.68		0.66	0.63
6	0.85	2.29[a]	2.47	1.77	2.39	2.68
7	0.82	1.43[a]	1.62		1.54	1.61
8	1.21	0.68	1.44		1.20	1.14

Note: ΔTg = temperature change in the girder, the girder bearing configuration = E---F/F---E/E---F, the length of the span = 80 ft, the length of the fastener = 30 in, and the temperature change in the rail = 60°F (temperature drop).

[a]Using average of Rf = $(n_sP_{fs} + n_{ns}P_{fns})/(N_s + n_{ns})$ where n_s = the number of slip fasteners, and n_{ns} = the number of nonslip fasteners.

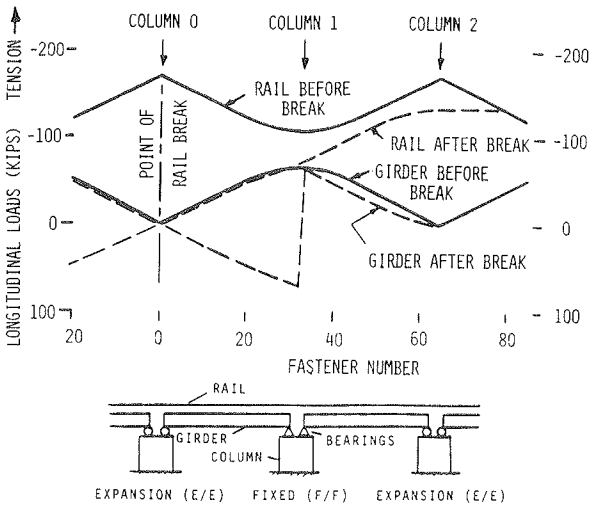

FIGURE 4 Typical force distributions on rails, girders, and columns.

structure (deck, girders) of an aerial guideway by differential movement and shear of the fasteners.

A typical axial force distribution diagram is given in Figure 4 for Case 1, the medium-restraint fastener. When a rail breaks, the substructure must then resist the unbalanced forces and moments transmitted through the girder bearings. Part of the load from the broken rail is transferred to the unbroken rail(s), and part is transferred to the substructure through fixed or expansion bearings. The exact magnitudes of these loads depend strongly on the substructure (bent or column) longitudinal stiffness, the structure bearing configuration, and the rail fastener restraint characteristics. The longitudinal stiffness of modern elevated guideway columns--depending on shape, dimensions, reinforcing steel, and, most importantly, column height--can typically range from 40,000 to 200,000 lb/in. Girder bearing stiffnesses act in series with the column stiffness, reducing the overall effective stiffness, even for fixed bearings.

An analysis of load transfer attributed to column stiffness was conducted, using an expanded version of TRKTHRM to account for the unbroken (but flexible) second rail. Results of the analysis for Case 1 (medium-restraint) and Case 4 (high-restraint) fasteners are given in Table 5. With even an effectively rigid (500,000 lb/in.) substructure, less than 40 percent of the broken-rail load on the first two girders is transferred to the column. Progressively lower loads are transferred to the columns as column stiffness decreases. Higher loads are, however, transferred to the unbroken rail, increasing the thermally induced stress in this rail and raising the possibility of a second break. Note that with high-restraint fasteners (Case 4), more load is transferred into the unbroken rail and less into the column than with medium-restraint fasteners (Case 1).

TABLE 5 Effects of Unbroken Rail and Column Longitudinal Stiffness on Loads Transferred to the Substructure

Column Stiffness (lb/in.)	Medium Restraint		High Restraint	
	Load (lb)	Gap Size (in.)	Load (lb)	Gap Size (in.)
Rigid	131,000	0.67	134,000	0.79
500,000	50,600	0.89	35,800	0.89
100,000	17,700	1.17	11,600	0.96
40,000	9,300	1.27	5,800	1.15

Note: Assuming a symmetrical girder bearing configuration of E---F/F---E/E---F, and a 60°F temperature drop.

PARAMETER VARIATION STUDIES

An analytical model was developed during this study to evaluate the more simple methods of predicting rail stresses and rail-break gap size. This program was expanded to account for structural compliances and the effects of the other, unbroken (but flexible) rails on the elevated transit structure. Basically, a relaxation method of solution is used in the model in which an initial solution based on rigid rail and structural elements is calculated, and the resulting loads are applied iteratively to the flexible elements until boundary conditions are satisfied.

An analysis of the effects of substructure (e.g., bent or column) longitudinal stiffness was conducted with the expanded model. Decreasing column stiffness was found to (a) increase rail gap size by as much as 90 percent over rigid-structure estimates, (b) increase the load transferred into the unbroken rail(s) and decrease the load transferred into the columns, and (c) increase column deflections.

A parameter variation study was then conducted to investigate the effects of different fastener stiffness and restraint characteristics using the three different girder bearing configurations of Figure 1. With unbroken rails, Configuration A (E---F/F---E/E---F) produced the highest loads into the girders and highest rail stresses, although Configuration B (E---E/E---E) produced the lowest loads and stresses. Configuration C (F---E/F---E/F---E) generally fell between the other two in load and stress magnitudes; however, because this configuration is nonsymmetrical, the girder loads are not balanced and must be reacted through the columns in bending. Reducing fastener longitudinal stiffness or slip force limit, or both, for a given configuration reduced the girder loads and rail stresses.

In the event of a rail break, girder bearing configuration was found to have little effect on the resulting rail gap size. Decreasing the fastener longitudinal stiffness or slip force limit, or both, increased the gap size, reduced load into the girder and the unbroken rail over the first girder, but increased loads transferred to subsequent girders. The asymmetric Configuration C produced the highest column bending loads on the fixed-bearing side of the rail break and these loads were substantially higher than the other two configurations for high-restraint fasteners. Configuration B, girders floating on expansion bearings, transferred the lowest loads into the columns. Configuration A transferred the least load to the girder, and more load to the unbroken rail, which was reflected in the highest unbroken rail stress of the three.

An older elevated transit structure was also modeled by the expanded computer code. This structure represented the proposed SEPTA reconstructed Frankford line with concrete deck, direct-fixation fasteners, and CWR track. The salient feature of the line is 231-ft-long girders supported on four rather compliant bent/column substructures. The proposed system will utilize high-restraint fasteners on one girder midway on a (maximum) 3,300-ft CWR string, with low-restraint fasteners used on the rest of the superstructure.

Results of this study show that the low-restraint fasteners do not adequately control the rail-break gap size. In addition, computer results showed that although rail stresses were increased as the low-restraint-fastener, slip-force limit was increased,

maximum girder longitudinal deflections were reduced, thus decreasing the loads into the columns. A medium-restraint fastener (2,500-lb slip-force limit) throughout the track structure could control the rail-break gap size and eliminate the need for rail expansion joints without producing exceptional rail stresses.

CONCLUSIONS

Current guideway design criteria were reviewed and compared in this study to assess their application to the use of CWR on elevated transit structures. The status of current design criteria and standards can be summarized as follows:

1. No specific criteria exist that govern the thermal interaction with CWR structures.
2. No technically justifiable guidelines exist for limiting the rail-gap size for rail breaks at low ambient temperatures.
3. Large variations exist in structural design methods from one transit system to another, leading to the conclusion that some systems may be overdesigned (hence cost inefficient), although others may have a lower factor of safety or (more likely) develop maintenance problems early in their lives.
4. Current methods of analysis range from simple formulas to complex finite-element models. The simpler methods are, for the most part, unreliable in predicting stresses and structural behavior critical to several major CWR-related design elements. These include (a) the control of stresses in rails attributed to thermally induced differential movements between rail and supporting structure, (b) the control of rail-break gap size and resulting loads into structures during low-temperature rail pull-apart failures, and (c) the transfer of thermally induced loads from the superstructure (deck and girder) through expansion bearings or fixed joints into the substructure (columns, piers, and foundations).
5. Decisions concerning CWR can have significant cost impacts on system construction. Based on a cost of $12 million/mi of elevated structure without CWR and thermal effects considered in the system design, the most conservative approach to design for CWR and thermal effects could increase structure costs by 23 percent. The least costly (though probably inadequate) design encountered increased structural costs by only 1 percent. Hence, a clear understanding of CWR behavior and of its implication on design criteria can substantially influence cost savings and performance.

The success of an operating system with aerial structures, DF fasteners, and CWR track is, to a large degree, a tribute to the successful application of particular design criteria. This success can be predicated to at least some degree, however, on component manufacturer, field construction and fabrication skills, and, eventually, maintenance practices. In this context, the BART track system (4) has been highly successful, and the system design criteria are therefore proven to be effective. In some features, however, the design may be overly conservative. The newer systems, such as MARTA and MDTA Metrorail, will hopefully prove to be equally as trouble-free.

ACKNOWLEDGMENTS

The authors wish to acknowledge the valuable contributions to this study by Henry G. Russell of Construction Technology Laboratories, Portland Cement Association, and Jeffrey A. Hadden of the Columbus Division, Battelle Northwest Laboratory. Thanks also to Karl Frese of Lee Wan Associates, Ed Jensen of Kaiser Transit Group, and Bertie Jackson of the Dade County Transportation Administration, as well as to the personnel of the five transit systems, for their generous assistance in this study.

REFERENCES

1. D.R. Ahlbeck, J.A. Hadden, H.G. Russell, A. Kish, and A. Sluz. CWR Design Criteria Assessment for Transit Structures. Final Report. Technical Task Directive 15. U.S. Department of Transportation, Jan. 1985.
2. B.W. Harrington, Jr. Investigation of Design Standards for Urban Rail Transit Elevated Structures. Report UMTA-GA-06-0010-81-1. UMTA, U.S. Department of Transportation, June 1981.
3. R.A. Dorton and H.N. Grouni. Review of Guideway Design Criteria in Existing Transit System Codes. ACI Journal, April 1978.
4. Rail-Structure Interaction Studies for Aerial Structures. Tudor Engineering Company, San Francisco, Calif., Nov. 1970.
5. Feasibility of Direct Track Fixation on Unballasted Structures, Appendix A: Interaction Between Rail and Structure on Unballasted Aerial Structures. De Leuw Cather and Company, Washington, D.C., March 1974.
6. Metropolitan Dade County Transportation Improvement Program Compendium of Design Criteria, Volume III--Guideways Design Criteria. Kaiser Transit Group, Miami, Fla., June 1978.
7. CWR/Aerial Structure Interface Report for Intermediate Capacity Transit Systems Vancouver ALRT Project. Parsons Brinckerhoff Centec, Vancouver, British Columbia, Canada, July 1982.
8. G.F. Fox. Design of Steel Bridges for Rapid Transit Systems. Presented at the 1982 Canadian Structural Engineering Conference.
9. P.W. Witkiewicz. A Survey of Direct Fixation Fastening Systems in North America: Existing Types and Associated Problems. Presented at 1983 Direct Fixation Fastener Workshop, Transportation Systems Center, U.S. Department of Transportation, Cambridge, Mass.
10. De Leuw, Cather and Company. Track Fasteners on the WMATA Metrorail System. Presented at 1983 Direct Fixation Fastener Workshop, Transportation Systems Center, U.S. Department of Transportation, Cambridge, Mass.
11. G.M. Magee. Calculation of Rail Bending Stress for 125 Ton Tank Car. Association of American Railroads Research Center, Chicago, Ill., April 1965.
12. W. So and G.C. Martin. Finite Element Track Buckling Model. Report T7-/RT-S. American Society of Mechanical Engineers, New York, April 1977.

Publication of this paper sponsored by Task Force on Rail Transit System Design.